MIT Libraries | DSpace@MIT

MIT Open Access Articles

Digital Signaling and Hysteresis Characterize Ras Activation in Lymphoid Cells

The MIT Faculty has made this article openly available. ***Please share*** how this access benefits you. Your story matters.

Citation: Das, Jayajit, Mary Ho, Julie Zikherman, Christopher Govern, Ming Yang, Arthur Weiss, Arup K. Chakraborty, and Jeroen P. Roose. "Digital Signaling and Hysteresis Characterize Ras Activation in Lymphoid Cells." Cell 136, no. 2 (January 2009): 337–351. © 2009 Elsevier Inc.

As Published: http://dx.doi.org/10.1016/j.cell.2008.11.051

Publisher: Elsevier

Persistent URL: http://hdl.handle.net/1721.1/96192

Version: Final published version: final published article, as it appeared in a journal, conference proceedings, or other formally published context

Terms of Use: Article is made available in accordance with the publisher's policy and may be subject to US copyright law. Please refer to the publisher's site for terms of use.

Massachusetts Institute of Technology

Cell

Digital Signaling and Hysteresis Characterize Ras Activation in Lymphoid Cells

Jayajit Das,[1,7] Mary Ho,[4] Julie Zikherman,[5] Christopher Govern,[1] Ming Yang,[1] Arthur Weiss,[5,6,*] Arup K. Chakraborty,[1,2,3,*] and Jeroen P. Roose[4,*]
[1]Department of Chemical Engineering
[2]Department of Chemistry
[3]Department of Biological Engineering
Massachusetts Institute of Technology, 77 Massachusetts Avenue, Cambridge, MA 02139, USA
[4]Department of Anatomy
[5]Department of Medicine, Division of Rheumatology
[6]Howard Hughes Medical Institute
University of California, 513 Parnassus Avenue, San Francisco, CA 94143, USA
[7]Present address: Battelle Center for Mathematical Medicine, Nationwide Children's Hospital and Department of Pediatrics, Biophysics Graduate Program, Ohio State University, 700 Children's Drive, Columbus, OH 43205, USA
*Correspondence: aweiss@medicine.ucsf.edu (A.W.), arupc@mit.edu (A.K.C.), jeroen.roose@ucsf.edu (J.P.R.)
DOI 10.1016/j.cell.2008.11.051

SUMMARY

Activation of Ras proteins underlies functional decisions in diverse cell types. Two molecules, RasGRP and SOS, catalyze Ras activation in lymphocytes. Binding of active Ras to SOS' allosteric pocket markedly increases SOS' activity establishing a positive feedback loop for SOS-mediated Ras activation. Integrating in silico and in vitro studies, we demonstrate that digital signaling in lymphocytes (cells are "on" or "off") is predicated upon feedback regulation of SOS. SOS' feedback loop leads to hysteresis in the dose-response curve, which can enable a capacity to sustain Ras activation as stimuli are withdrawn and exhibit "memory" of past encounters with antigen. Ras activation via RasGRP alone is analog (graded increase in amplitude with stimulus). We describe how complementary analog (RasGRP) and digital (SOS) pathways act on Ras to efficiently convert analog input to digital output. Numerous predictions regarding the impact of our findings on lymphocyte function and development are noted.

INTRODUCTION

Activated Ras proteins regulate several cellular processes by acting on many substrates to affect signaling through diverse pathways (e.g., the MAPK pathway) (Campbell et al., 1998; Mor and Philips, 2006). Membrane-bound Ras proteins shuttle between inactive (GDP-bound) and active (GTP-bound) states. RasGDP binding to guanine nucleotide exchange factors (GEFs) results in nucleotide release, enabling nucleotide-free Ras to bind more abundant cellular GTP (Campbell et al., 1998). The intrinsic GTPase activity of Ras is enhanced by Ras GTPase-activating proteins (RasGAPs) that promote Ras deactivation (Campbell et al., 1998).

Ras activation is important for the development of T and B lymphocytes and for their effector functions directed against invading pathogens (Genot and Cantrell, 2000). Antigen receptor stimulation of lymphocytes triggers uniquely high levels of Ras activation (Genot and Cantrell, 2000). Two families of RasGEFs are well studied in lymphocytes: RasGRP1 and RasGRP3 (Ras guanyl nucleotide release protein) and SOS1 and SOS2 (Son of Sevenless) (Ebinu et al., 2000; Roose et al., 2005, 2007). RasGRP proteins, mainly restricted to the nervous and hematopoietic systems, are activated by binding to membrane-localized diacylglycerol and by phosphorylation by protein kinase C (see Figures 2A and 4A). SOS proteins are ubiquitous and are recruited to sites of receptor or adaptor tyrosine phosphorylation. SOS' activity is regulated by membrane localization and is greatly accelerated upon binding of active RasGTP to a noncatalytic (allosteric) site (Margarit et al., 2003). The functional consequences of such feedback regulation of SOS' activity, and its interplay with the other GEF, RasGRP, were unknown.

An important issue in cell biology is to understand how cells respond in a decisive manner (digital) to the graded (analog) input of increasing amounts of receptor stimulation. Employing synergistic in silico and in vitro methods, we find that signaling in a population of lymphocytes is digital in character, i.e., a bimodal response emerges as stimulus is increased past a threshold. Digital signaling in individual cells requires SOS-mediated Ras activation. A further unanticipated characteristic of Ras activation via SOS is hysteresis in the dose-response curve, i.e., the response to the same stimulus dose depends upon whether the prevailing level of stimulus is achieved by increasing or decreasing the stimulus from its previous value. Our results

suggest that bimodal responses and hysteresis also provide a mechanism for short-term molecular "memory," making it easier to activate membrane-proximal signaling in previously stimulated cells. This may enable T lymphocytes to integrate signals from serial encounters with rare antigen-bearing cells.

We find that Ras activation via RasGRP alone increases in a graded fashion with stimulus (analog) and does not exhibit hysteresis. This is because, unlike SOS, RasGRP's activity is not regulated by a positive feedback loop. Our results show how tuning the interplay between two complementary digital and analog signaling modules that activate the same substrate (Ras) leads to more efficient digital responses than if the digital pathway alone was employed. This may be a principle used broadly in biology.

Positive feedback regulation is one of many nonlinear mechanisms that can result in "digital" responses of gene regulation programs and signaling networks (Barkai and Leibler, 2000; Bhalla and Iyengar, 1999; Elf and Ehrenberg, 2004; Ferrell, 2002; Kholodenko et al., 2002; Kussell et al., 2005; McAdams and Arkin, 1997). We describe an example of how positive feedback regulation of a signaling module embedded in a complex signaling network leads to functionally important consequences in cells that orchestrate adaptive immunity. The concepts revealed by our study lead to a number of testable predictions pertinent to lymphocyte development and their ability to be activated in vivo by small doses of stimulatory ligands.

RESULTS

A Positive Feedback Loop that Regulates SOS Activity Results in Digital Signaling

Stimulated tyrosine kinase receptors (e.g., growth factor receptors, T cell receptors) recruit SOS to the plasma membrane by the adaptor molecule, Grb2 (Genot and Cantrell, 2000). The Rem and Cdc25 domains in SOS are required for its GEF catalytic activity (Figure 1A), and we refer to them together as SOS_{cat} (SOS catalytic domain). SOS itself has very low GEF activity. Crystallographic and biochemical studies as well as experiments with cell lines show that the activity of SOS_{cat} is strongly influenced by a second Ras binding site that is distal to the GEF catalytic site (Margarit et al., 2003). Binding of RasGDP to this allosteric pocket results in a 5-fold increase in GEF activity, whereas binding of RasGTP effects a much larger (~75-fold) increase (Freedman et al., 2006; Sondermann et al., 2004). Thus, SOS-mediated Ras activation involves positive feedback regulation by its own catalytic product, RasGTP (Figure 1A).

The activity of full-length SOS is inhibited by both N-terminal and C-terminal regions that flank SOS_{cat} (Figure S21A available online). Recruitment of SOS to the plasma membrane results in conformational changes that relieve this inhibition and allow RasGDP to bind to SOS' catalytic site (Corbalan-Garcia et al., 1998). Binding of membrane phosphatidylinositol-4,5-bisphosphate (PIP_2) to SOS' N-terminal PH domain further augments SOS' activity (Gureasko et al., 2008). In agreement, expression of $SOS1_{cat}$ without these flanking sequences results in Ras signaling without the need for membrane targeting or external stimulus (Roose et al., 2007). We explored the consequences of positive feedback regulation of SOS by developing a mathematical model for the signaling module in Figure 1B wherein SOS_{cat} is uninhibited.

We first ignored stochastic fluctuations (van Kampen, 1992) in the number of molecules participating in signaling and developed a deterministic model describing the temporal evolution of the most probable number (or concentration) of the proteins involved in Ras activation via SOS_{cat} (Figure 1B). Table 1 summarizes the values of rate parameters that appear in the equations (Experimental Procedures). Only the ratios of certain parameters had been measured. Varying the individual parameters by factors of at least ten while keeping the ratio fixed did not affect the qualitative results (Figures S2–S4).

Figure 1C shows the theoretical steady-state dose-response curve for Ras activity as the amount of SOS_{cat} (α) is varied. For low or high levels of SOS_{cat}, there is one possible state characterized by low or high levels of active Ras, respectively. However, for intermediate levels of SOS_{cat}, three states of Ras activity are possible. The states shown in blue are unstable to small perturbations, and these states could exist only fleetingly. Therefore, for intermediate levels of SOS_{cat}, two possible dominant states of Ras activity could be simultaneously observed, i.e., a bistability is predicted. As the amount of SOS_{cat} is increased, the system could follow the lower stable branch until this was no longer possible, and then there would be a large jump in Ras activity (at point A). Thus, the dose-response curve could be very sharp. Importantly, bistability and the concomitant sharp threshold are abrogated if the positive feedback loop regulating SOS' GEF activity is removed from the model (green line in Figures 1D and S2E).

Formulas obtained from a detailed analytical study (Supplemental Data, Section VI) suggest that, in addition to feedback regulation of SOS, the minimal requirements for bistable Ras activity are (1) catalytic Ras activation by SOS, with RasGTP bound to the allosteric site and (2) catalytic deactivation of RasGTP by RasGAPs. These features are true. The analytical treatment of simplified models also supports our numerical parameter sensitivity studies, which show that our qualitative results are robust to wide variations in parameters as long as the basic ingredients described above are present.

We then investigated the potential effect of Ras activation via RasGRP1 on the bistable Ras activity driven by SOS_{cat}. A GEF, RasGRF, which is structurally related to RasGRP, is not dependent on feedback regulation by Ras (Freedman et al., 2006). So, we assumed that Ras is activated by RasGRP without feedback and used the measured rate parameters for RasGRF since those for RasGRP are unknown. As shown in Figure 1E, bistability and sharp responses are predicted to disappear if RasGRP levels (or activity) are very high. This is because RasGRP activity, which is not subject to feedback regulation, can convert most Ras molecules to its active form before the SOS feedback loop is engaged. Figure 1E also shows that low levels of RasGRP activity reduce the threshold for SOS_{cat} (α) to induce a sharp response. We show later that this is because absence of RasGRP makes it difficult to ignite the positive feedback loop regulating SOS' GEF activity. These results suggest that an optimal level of expression or activity of RasGRP, the analog route to Ras activation, enables efficient deployment of feedback regulation of SOS, which leads to bistability.

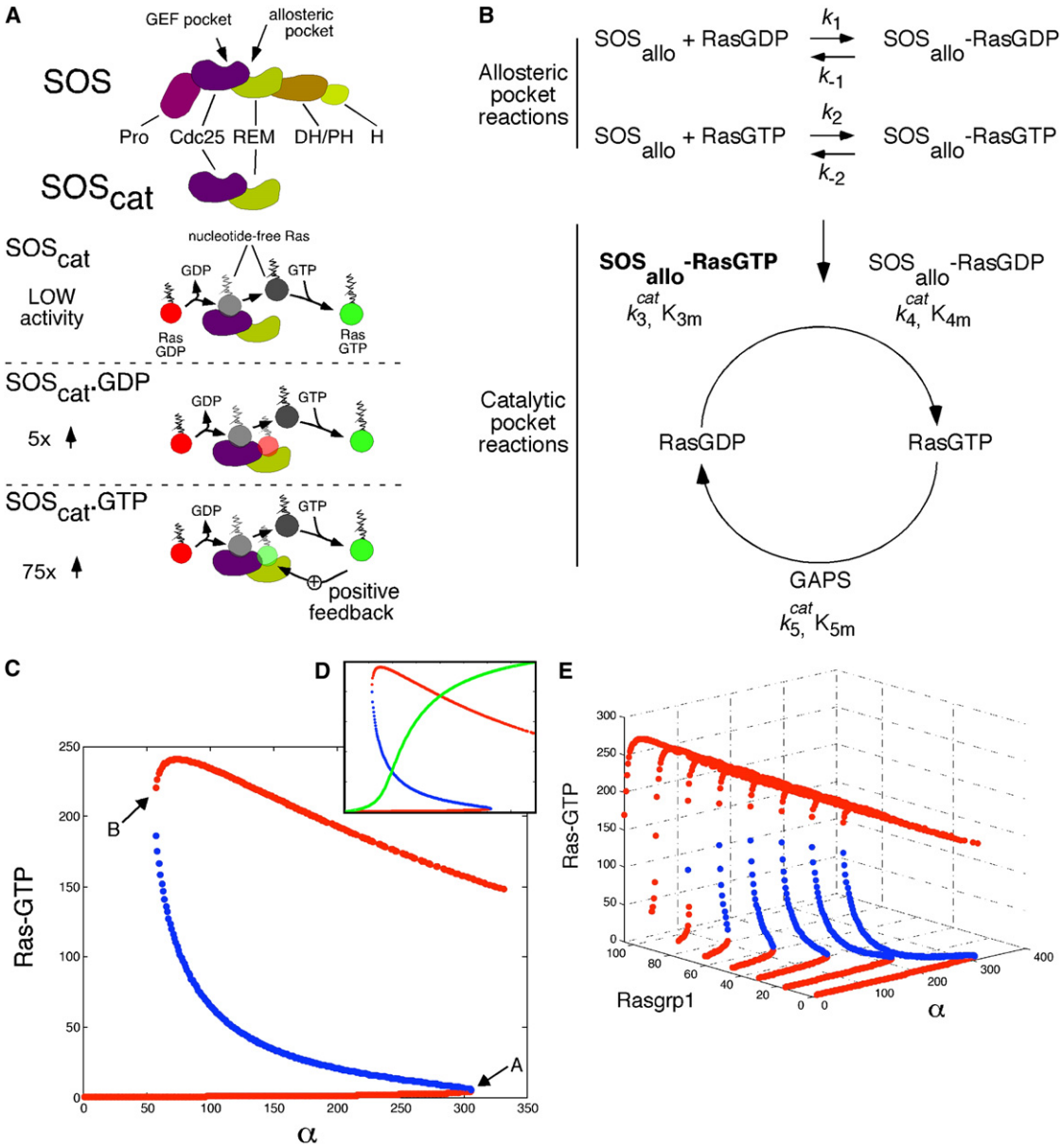

Figure 1. A Minimal Model of the Catalytic Domain of SOS Predicts Three Possible States of Ras Activation

(A) SOS' protein domains, GEF pocket, and allosteric pocket. Pro = proline-rich; Cdc25 = Cdc25 homology domain; REM = Ras exchange motif; DH/PH = Dbl-homology, Pleckstrin-homology domain; H = histone folds. SOS_{cat} includes the catalytic region that contains both the GEF and the allosteric pockets. Illustration of SOS_{cat}'s mode of Ras activation. Binding of RasGTP to the allosteric pocket increases SOS_{cat}'s activity 75-fold, establishing a positive feedback loop.

(B) Depiction of the allosteric pocket and catalytic site reactions on SOS_{cat}. SOS_{allo}-RasGTP in bold reflects the 75-fold increased catalytic activity.

(C) Steady states of the mean-field kinetic rate equations show production of low and high concentrations of RasGTP (characterized by stable fixed points in red) at low and high values of α. α represents the total number of SOS_{cat} molecules in the simulation box (see Supplemental Data, Section I). At intermediate levels of α, three states arise with unstable fixed RasGTP points shown in blue.

(D) Overlay with analysis in (C). The green line represents simulations when the allosteric pocket of SOS_{cat} is mutated in a way that it cannot bind to RasGDP or RasGTP. In order to demonstrate the overlay in the same graph, the low catalytic rate (kcat $\sim$0.0005 s^{-1}) of the mutant SOS_{cat} was artificially increased to 0.038 s^{-1}.

(E) Steady-state activation of RasGTP as a function of SOS_{cat} and RasGRP. The RasGRP-DAG complex (abbreviated RasGRP) catalyzes RasGDP following the reactions shown in reaction #8 in Table S4. This reaction is incorporated in the ODE model: $k_8^f[RasGRP-DAG][Ras-GDP]/(K_{8m}+[Ras-GDP])$, in Equation 1C with $k_8^f = 0.01 s^{-1}$ and $K_{8m} = 3.06\ \mu M$, calculated from Table S4. Unstable and stable points are shown in blue and red, respectively.

To explore the manifestations of these characteristics of Ras activation in lymphocytes (where stochastic variations between stimulated cells can be important), we carried out stochastic computer simulations of signaling events that might occur in lymphocytes (Figure 2A). The simulations were carried out using the Gillespie algorithm (Gillespie, 1977), which has been used

Table 1. Rate Constants Used for Model in Figure 1

k_1	k_{-1}	k_2	k_{-2}	k_3^{cat}	K_{3m}	k_4^{cat}	K_{4m}	k_5^{cat}	K_{5m}
1.8×10^{-4} $(\mu m)^3(mols)^{-1}s^{-1}$	$3.0\ s^{-1}$	1.7×10^{-4} $(\mu m)^3(mols)^{-1}s^{-1}$	$0.4\ s^{-1}$	$0.038\ s^{-1}$	1.64×10^3 $(mols)/(\mu m)^3$	$0.003\ s^{-1}$	9.12×10^3 $(mols)/(\mu m)^3$	$0.1\ s^{-1}$	1.07×10^2 $(mols)/(\mu m)^3$
Sondermann et al., 2004	Sondermann et al., 2004	Sondermann et al., 2004	Sondermann et al., 2004	Freedman et al., 2006	Sondermann et al., 2004; Freedman et al., 2006	Boykevisch et al., 2006	Sondermann et al., 2004; Boykevisch et al., 2006	Gideon et al., 1992; Trahey and McCormick, 1987	Gideon et al., 1992; Trahey and McCormick, 1987

Parameters used for the equations. Rates are calculated from the catalytic rates and/or the dissociation constants (K_D) reported in the literature. For additional information, see Supplemental Data, Section I.

profitably to study biological systems that exhibit multistability (Elf and Ehrenberg, 2004; Kussell et al., 2005; McAdams and Arkin, 1997). Parameters not listed in Table 1 needed to carry out the simulations are provided in the Supplemental Data. The qualitative features of the results are robust to variations in unknown parameters over wide ranges (Tables S6–S8, Figures S5–S12). The purpose of our in silico studies was not quantitative recapitulation of known data but to provide qualitative mechanistic insights that can be tested experimentally.

We carried out stochastic calculations using the amount of SOS_{cat} as a surrogate for the level of receptor stimulation. Many replicate dynamic simulations were carried out and levels of RasGTP at various time points were recorded (see Figure S30 for examples). Each simulation corresponds to assaying an individual lymphocyte. The combined results for all such in silico "cells" at a particular time point are displayed (Figure 2B). For low levels of SOS_{cat}, all simulations result in low levels of RasGTP, resulting in a single corresponding peak in the histogram. As SOS_{cat} is increased, this peak does not gradually move to higher values of RasGTP. Rather, beyond a threshold value of SOS_{cat}, a second peak corresponding to a much higher level of RasGTP emerges; the histogram is bimodal (Figure 2B). Thus, the sharp threshold and bistability shown in Figure 1C are manifested as digital signaling. The prediction is that lymphocytes are either "on" or "off" with regard to Ras activation.

To test these predictions, we used a Jurkat T cell line into which different amounts of $SOS1_{cat}$ and GFP were transfected together (Roose et al., 2007). Individual cell assays are required to compare experimental results with the histograms shown in Figure 2B. Analysis of active Ras for individual cells in a population is not possible in this transfection experiment, and so we examined upregulation of a cell-surface activation marker CD69 by individual cells using flow cytometry. CD69 levels correlate with the strength of Ras-ERK signaling (Roose et al., 2007), but activation of signaling molecules downstream of Ras could be influenced by feedback regulation of modules such as the MAPK pathway (Ferrell, 2002; Kholodenko et al., 2002). We will address this issue directly below.

Low or high levels of $SOS1_{cat}$ expression led to unimodal cell populations with low or high levels of CD69 induction (Figures 2C and S21B). Intermediate levels of $SOS1_{cat}$ (red) induced a bimodal CD69 expression pattern in wild-type (WT) Jurkat T cells (Figure 2C). $SOS1_{cat}$-induced bimodality was not observed for a control marker that is Ras unresponsive (Figure S21C). These results in cells mirror the predictions of the computer simulations in that signaling is digital. We next tested the hypothesis emerging from our calculations (Figures 1C and S2E) that the origin of digital signaling is feedback regulation of SOS-mediated Ras activation.

Experiments carried out with RasGRP1-deficient JPRM441 cells indicate the importance of this feedback loop. In contrast to WT cells (Figure 2C), intermediate levels of $SOS1_{cat}$ induced high CD69 expression levels in very few JPRM441 cells (13% in Figure 3A, top row). Similarly, intermediate levels of SOS_{cat} did not generate a bimodal response in computer simulations of the RasGRP-deficient state (Figure 3B). Basal RasGRP1-mediated activation of Ras is not subject to feedback regulation but can "ignite" the SOS feedback loop (Roose et al., 2007) by providing RasGTP that can bind SOS' allosteric pocket and increase its activity 75-fold. Consistent with our computational results (Figure 1E), in RasGRP-deficient JPRM441 cells, lower basal levels of RasGTP make it more difficult to ignite the SOS feedback loop. Sufficiently high levels of SOS_{cat} can induce bimodal responses without RasGRP1 (Figures 3A, 3B, 1E, and S22) because RasGTP produced by the GEF activity of SOS_{cat} with RasGDP bound to the allosteric pocket can ultimately prime SOS' feedback loop.

The computer simulation results suggested that a bimodal response would re-emerge in RasGRP-deficient cells for intermediate levels of $SOS1_{cat}$ if exogenous RasGTP molecules that bind to SOS' allosteric pocket were added. To test this, we introduced Ras molecules like H-RasV12C40 (Roose et al., 2007) or H-RasG59E38 (Boykevisch et al., 2006) that are predominantly GTP loaded (because of the V12 or G59 mutation) and thus bind SOS' allosteric pocket to increase GEF activity. These molecules also contain a second mutation (C40 or E38) that impairs binding to RAF and so do not directly activate the RAF-MEK-ERK-CD69 pathway, i.e., downstream pathways must be activated by endogenous Ras molecules.

In this type of assay, not all transfected cells start to express $SOS1_{cat}$ synchronously and $SOS1_{cat}$-expressing cells transit from low CD69 to high CD69 expression. It is therefore difficult to ascertain whether the response is bimodal or not by visual inspection. We adapted Hartigan's test (Hartigan and Hartigan, 1985), which allows for a qualitative determination of whether a response in a population of cells is bimodal or unimodal. The generated histograms were divided into 120 equal portions and the mean fluorescence of CD69 and the number of cells in each portion were determined. Hartigan's test confirmed that intermediate levels of $SOS1_{cat}$ when combined with H-RasG59E38, but not with WT H-Ras, restored bimodal signaling

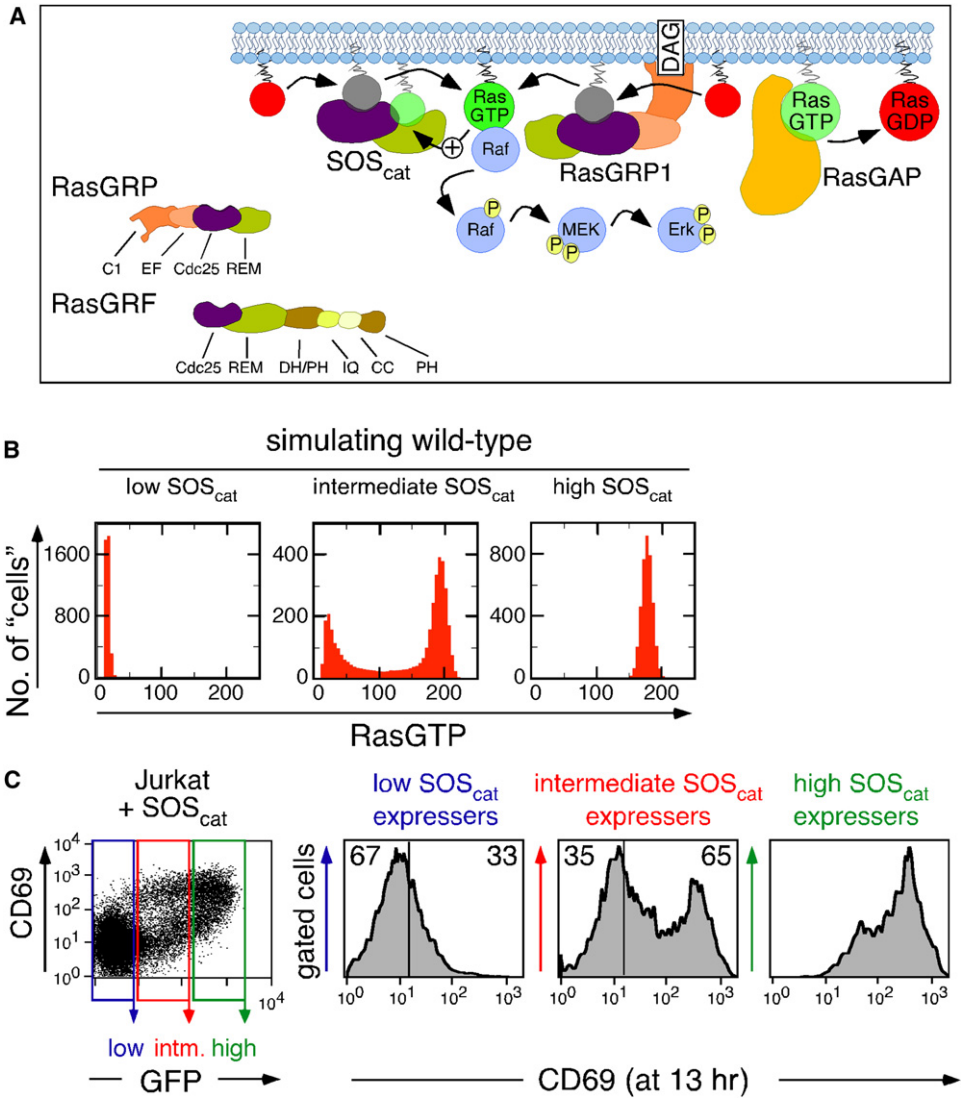

Figure 2. Bimodal Ras Activation Induced by SOS$_{cat}$ Operating in the Ras Signaling Network Occurs in a Stochastic Model and in a T Cell Line

(A) Representation of SOS$_{cat}$ function in the context of the Ras signaling network. Besides SOS1 and 2, lymphocytes express the RasGEFs RasGRP1 and 3 and RasGRF2. C1 = DAG-binding C1 domain, EF = calcium-binding EF hand, IQ = motif for calcium/calmodulin binding, CC = coiled coil. RasGTP produced by RasGRP1 can influence SOS' activity via the allosteric pocket. Of note, deficiency of RasGRF2 does not appear to impact T cell Ras activation but influences the calcium-NFAT pathway (Ruiz et al., 2007).

(B) Distributions of RasGTP calculated from our stochastic simulation algorithm at low, intermediate, or high levels of SOS$_{cat}$ (2-fold increments) in a wild-type (WT) "cell." At intermediate levels of SOS$_{cat}$ a bimodal RasGTP pattern arises. See Section II (Tables S4–S8, Figures S5–S12) for additional information.

(C) Introduction of intermediate levels of SOS1$_{cat}$ into a WT Jurkat T cell line leads to bimodal upregulation of CD69. Cells were cotransfected with 10 μg of GFP- and 10 μg of SOS1$_{cat}$ -expressing plasmid. Dot plots depict CD69 and GFP expression on individual cells, analyzed by FACS. Electronic gates define low, medium, and high GFP expression, reflecting low, medium, and high expression of the cotransfected SOS1$_{cat}$ plasmid. CD69 expression was analyzed in histograms for the three different gates. See Figure S21B for protein expression levels. (C) is a representative example of three independent experiments.

in RasGRP-deficient cells (Figure 3C, bottom row: Bimodal with $p < 0.01$). The same level of SOS1$_{cat}$ or H-RasG59E38 alone also did not result in high CD69 expression (Figure 3C, top row, unimodal; U:p < 0.01). Importantly, when the allosteric pocket in SOS$_{cat}$ is mutated (SOS1$_{cat}$-W729E), so that it can no longer interact with nucleotide-associated Ras proteins, adding H-RasG59E38 does not result in a bimodal pattern of signaling (Figure 3C, bottom row). Similar results were obtained with H-RasV12C40 (data not shown). Modeling Ras activation in this cell biological experiment is in concurrence with these results (Figure 3D). Therefore, the digital signaling we observe for ERK-CD69 signaling requires feedback regulation of SOS-mediated Ras activation.

There are two possible reasons for why digital signaling in lymphocytes originates in SOS-mediated Ras activation: (1) Ignition of the SOS feedback loop is necessary for generating

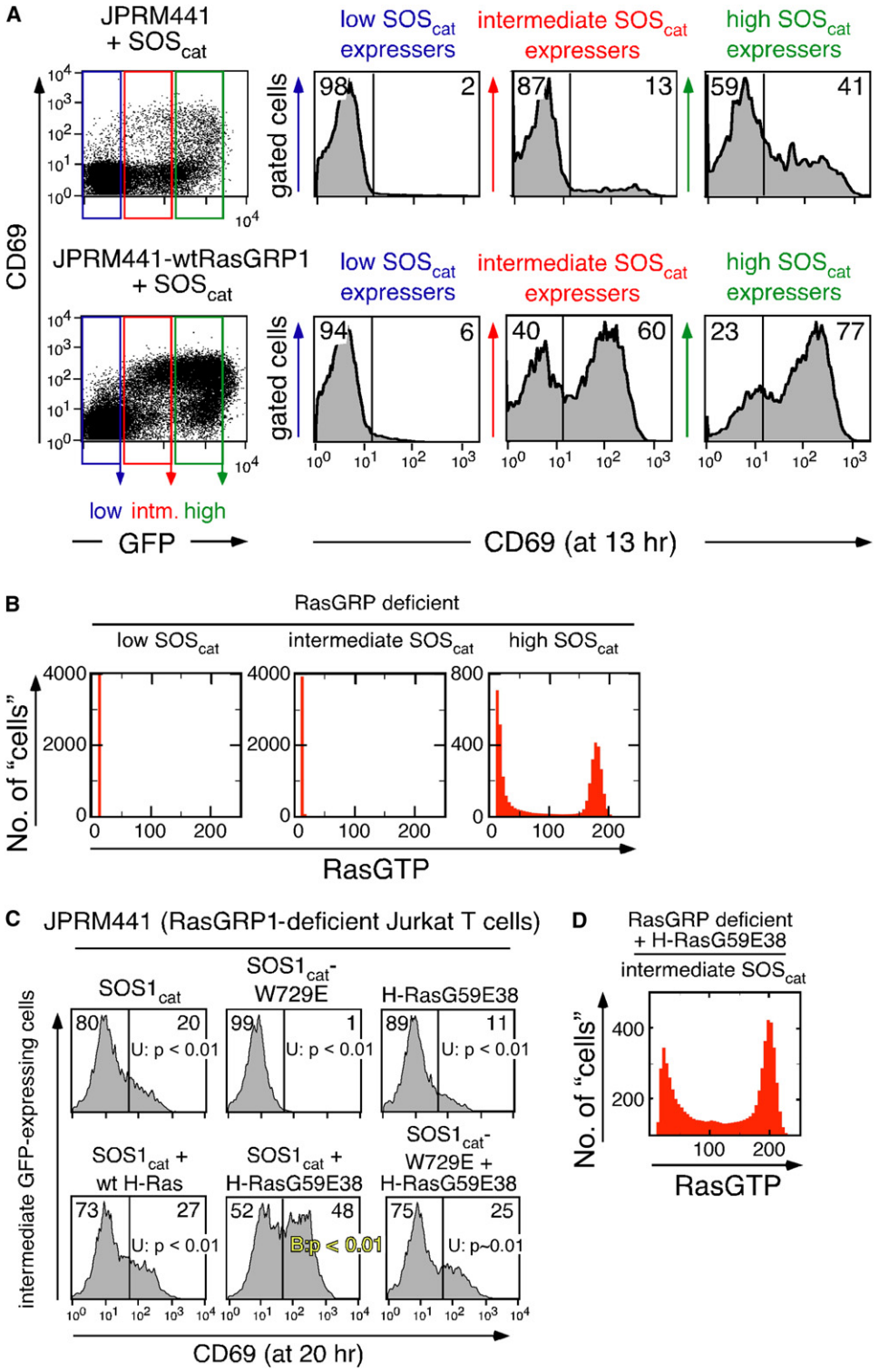

Figure 3. A RasGTP Mimetic Restores Efficient SOS_{cat}-Induced Bimodal Signals in RasGRP-Deficient Cells

(A) Analysis of the efficiency of SOS_{cat}-induced Ras signaling in a RasGRP1-deficient Jurkat T cell line (JPRM441) and its WT RasGRP1-reconstituted derivative line (JPRM441-WTRasGRP1). Experimentation and analysis as in Figure 2C, see also Figure S21B. Intermediate SOS_{cat} induces high levels of CD69 expression in only 13% of the JPRM441 cells. This relative defect in JPRM441 cells is restored to 60% in the JPRM441-WTRasGRP1 cells.

(B) Stochastic simulations as in Figure 2B. Histograms of RasGTP simulating a RasGRP-deficient state are depicted. Increments of SOS_{cat} between the plots are 2-fold. Note the lack of a bimodal distribution in "cells" with intermediate SOS_{cat}.

sufficiently high levels of RasGTP required to prime downstream feedback loops that cause digital signaling (e.g., those associated with the MAPK pathway [Bhalla and Iyengar, 1999; Ferrell, 2002; Kholodenko et al., 2002]). (2) Digital signaling is controlled by feedback regulation of Ras activation by SOS. Whereas signaling is undoubtedly influenced by feedback regulation of downstream signaling modules, results described below suggest that, in lymphocytes, the latter scenario is true.

Receptor Stimulation Results in Digital Signaling with SOS and Analog Responses with RasGRP Alone

The strength of lymphocyte receptor stimulation impacts outcomes (e.g., T cell activation, thymocyte development; Starr et al., 2003). Therefore, we studied how SOS and RasGRP influence cellular responses as the amount of stimulatory ligands is varied.

We studied a simplified computational model for processes upstream of Ras activation (See Section III, Supplemental Data). In short (see Figure 4A), receptor stimulation and phosphorylation generate activated ZAP-70 molecules. Activated ZAP-70 phosphorylates the adaptor molecule LAT, which recruits both PLCγ and Grb2/SOS. PLCγ is then phosphorylated, and this generates IP3 and DAG. Induced DAG enhances RasGRP recruitment and activation. We do not incorporate cooperative effects associated with Grb2/SOS recruitment to LAT (Houtman et al., 2006). Including this feature would lead to sharper cellular responses (Prasad et al., 2009).

For weak receptor stimulation, as might occur under physiologic antigen receptor stimulation (Figure 4B), WT systems that have low initial levels of active Ras exhibit a bimodal pattern of signaling after a short time that ultimately becomes a unimodal distribution with high RasGTP (Figure 4B, left column). For very strong stimulation, a unimodal state of high RasGTP is rapidly reached (Figure 4C, left column). Without RasGRP, signaling is inhibited. Importantly, without SOS such systems demonstrate a graded response, indicating the analog character of RasGRP-mediated Ras activation (Figure 4C, middle column). Changing the values of the parameters (e.g., the numbers of RasGRP and SOS molecules) used to obtain the results shown in Figure 4 does not lead to qualitative changes (Tables S12 and S13, Figures S13–S20).

To test these predictions, we determined the pattern of ERK phosphorylation in individual cells. First, 20,000 Jurkat T cells were either stimulated via the T cell receptor (TCR) or by phorbol myristate acetate (PMA). The latter mimics a DAG-PKC-RasGRP pathway but does not target SOS. Engagement of the TCR generated a unimodal P-ERK response at early time points that transitioned to a bimodal response at 3 min after stimulation (Figure 5A). In contrast, even strong stimulation via PMA never induced a bimodal ERK phosphorylation pattern and, instead, exhibited an analog response (Figure 5B).

Experiments with cells wherein genes of interest were deleted further support these results. Peripheral T cells do not develop in RasGRP1-deficient mice (Dower et al., 2000), and a selective $SOS1^{-/-}SOS2^{-/-}$ peripheral T cell model to circumvent lethality due to SOS1 deficiency has not been generated (Wang et al., 1997). Therefore, we used a chicken DT40 B cell line in which pertinent genes have been genetically inactivated (Oh-hora et al., 2003). We analyzed the ERK phosphorylation pattern of 20,000 cells (WT, $SOS1^{-/-}SOS2^{-/-}$, and $RasGRP1^{-/-}RasGRP3^{-/-}$) that were stimulated with increasing levels of B cell receptor (BCR) crosslinking-M4 monoclonal antibody.

WT cells stimulated by low levels of M4, mimicking physiological lymphocyte stimulation by antigen, exhibited a bimodal pattern of ERK activation at the 3 and 10 min time points (Figure 5C "WEAK" and Figure S24). Hartigan's tests (Hartigan and Hartigan, 1985) confirmed that the response is bimodal. In contrast, $SOS1^{-/-}SOS2^{-/-}$ DT40 B cells did not exhibit bimodal distributions at any time point regardless of stimulus level (Figure 5C, middle column). Thus, without SOS, signaling is analog in character regardless of strength of stimulus. Furthermore, while PMA-induced responses were severely impaired in $RasGRP1^{-/-}$ $RasGRP3^{-/-}$ cells (Figure 5D, right column), PMA induced very similar analog patterns of ERK phosphorylation in WT and $SOS1^{-/-}SOS2^{-/-}$ DT40 B cells (Figure 5D, left and middle columns). These results reveal analog ERK responses from RasGRP-induced Ras activation, and that there is no intrinsic defect preventing $SOS1^{-/-}SOS2^{-/-}$ DT40 B cells from turning on the Ras-ERK pathway.

This behavior in cell lines was mirrored in primary CD4-positive peripheral T cells. Ex vivo TCR stimulation of primary cells results in a digital pattern of ERK phosphorylation (Figure 5E), but PMA stimulation results in analog signaling (Figure 5F).

Thus, in Jurkat T cells, DT40 B cells, and primary lymph node T cells digital signaling requires engagement of the SOS pathway for Ras activation (Figures 2–5). Notably, for all systems, the ERK response to PMA stimulation was analog at all doses tested, including those that generate high levels of RasGTP. This implies that the predicted analog Ras response in the absence of SOS (Figure 4C, middle column) is not translated to digital responses by downstream signaling modules. If ignition of the positive feedback loop associated with SOS-mediated Ras activation only served to generate high levels of RasGTP that can stimulate digital signaling in a downstream module such as the MAPK pathway, a bimodal pattern of ERK activation should have been observed upon strong PMA stimulation. Since this is not so (Figures 5B and 5D), our results suggest that the digital signaling we observe for ERK and CD69 is not only predicated on positive feedback regulation of SOS-mediated Ras activation (Figures 3 and 4C) but is controlled by it.

(C) Introduction of a RasGTP mimetic overcomes RasGRP1 deficiency in JPRM441 cells. JPRM441 cells were transfected with GFP together with SOS_{cat}, SOS_{cat}-W729E (allosteric pocket mutant), H-RasG59E38 (RasGTP mimetic), H-Ras, or combinations thereof. CD69 expression was analyzed by FACS and depicted as histograms for the intermediate GFP-expressing cells. Histograms were subsequently analyzed by a Hartigan's statistical test to examine uni- versus bimodality. See Figure S24. H-RasG59E38 synergizes with SOS_{cat} to produce a bimodal pattern (Hartigan's test; Bimodal: $p < 0.01$) but not with SOS_{cat}-W729E. For detailed description and expression levels of introduced proteins see Figure S23. Figure 3C is representative of results in three independent experiments.

(D) Stochastic simulations introducing an H-RasG59E38 molecule into the mathematical model. Note the reappearance of a bimodal response in "cells" with intermediate SOS_{cat}, compared to (B).

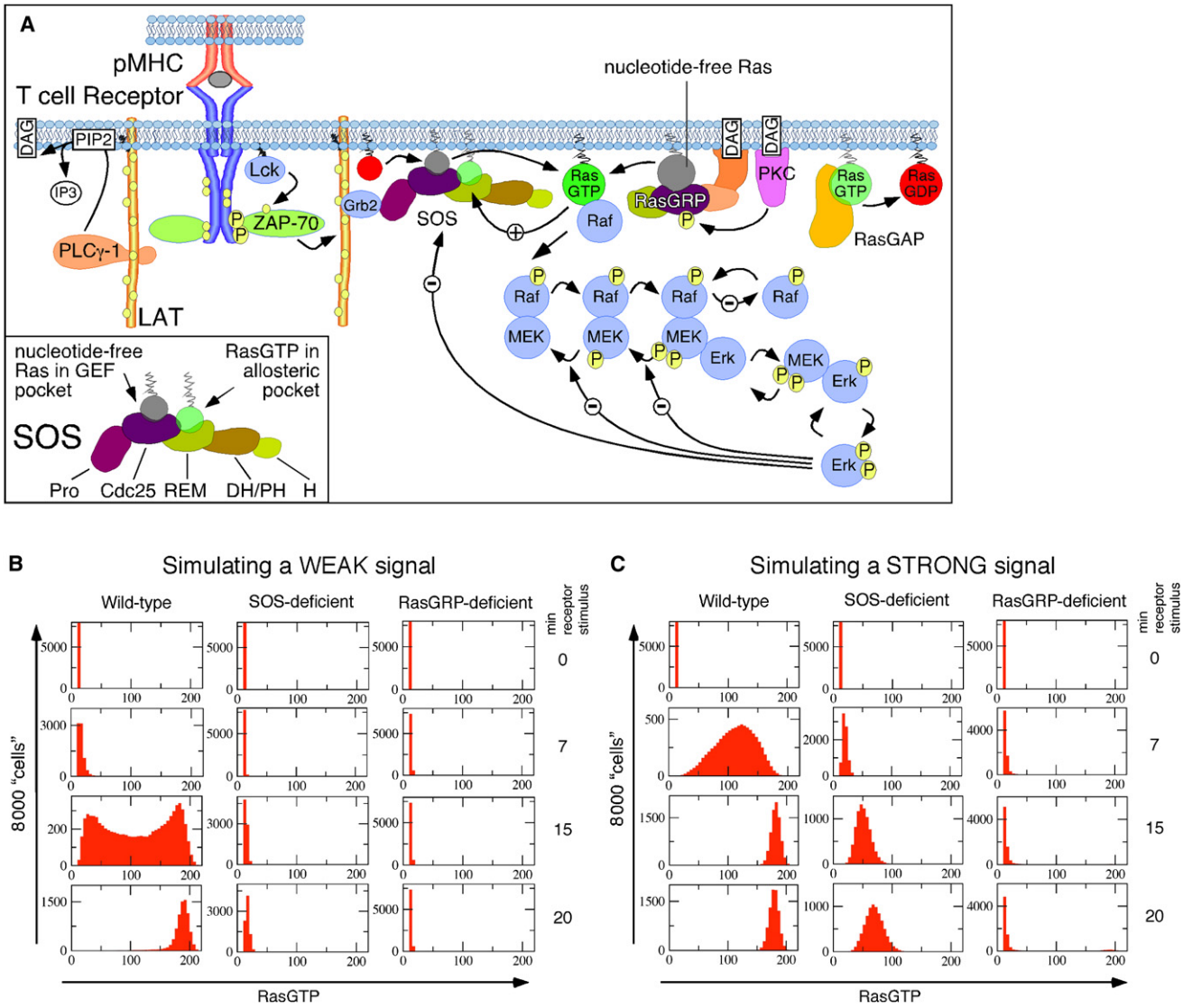

Figure 4. Digital Antigen Receptor Induced Ras Activation In Silico

(A) Representation of the Ras signaling network in T lymphocytes that is simulated by our stochastic simulation algorithm. Lck phosphorylates TCRζ leading to recruitment of ZAP-70. ZAP-70 phosphorylates LAT resulting in the recruitment of Grb2-SOS and PLCγ1. DAG produced by PLCγ1 leads to phosphorylation of RasGRP1 by PKCθ. Both SOS and RasGRP produce RasGTP signaling downstream to RAF, MEK, and ERK. B lymphocytes express PLCγ2 and downstream signaling events are very similar to those in T lymphocytes.

(B) Ras activation in 8000 "cells" in simulation induced by weak receptor signals over time. A bimodal RasGTP pattern emerges in WT but not SOS- or RasGRP-deficient states.

(C) Same as in (B) but simulating strong receptor signals. RasGTP levels rapidly increase in the WT "cells." A graded increase in RasGTP is observed in the SOS-deficient system. See Supplemental Data, Section III (Tables S9–S13, Figures S13–S20) for additional information, parameters, and parameter variation tests.

Prediction of Hysteresis in Ras Activation

Due to technical limitations, we are not able to carry out single-cell assays of Ras activity. However, another related, but unanticipated characteristic that derives from our model, hysteresis, can be assessed by measuring Ras activation at the population level. Hysteresis is a direct consequence of bistability due to positive feedback regulation of SOS-mediated Ras activation (Figure 1), and the phenomenon and its biochemical origin are shown in Figure 6.

When previously unactivated cells are stimulated, RasGTP levels are low. Hence, the allosteric site of most SOS molecules is occupied by RasGDP and SOS' GEF activity is low. Increasing stimulus results in more RasGTP production and an increase in the number of SOS molecules with RasGTP bound to the allosteric pocket, resulting in ignition of the positive feedback loop and a sharp increase in active Ras levels. These processes result in the black dose-response curve in Figure 6A, which is obtained from computer simulations where the initial RasGTP levels are set to zero.

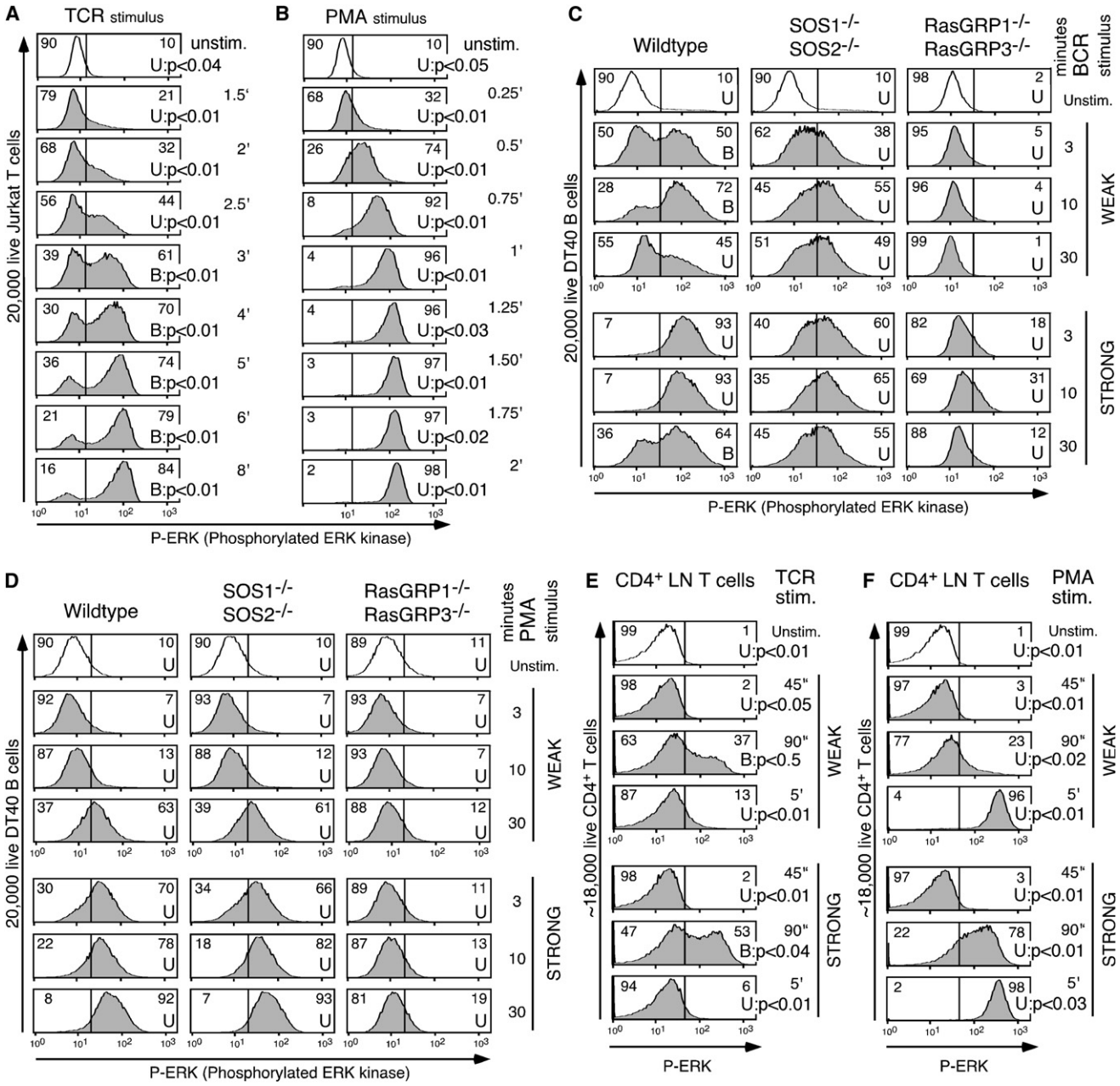

Figure 5. RasGRP Induces Analog Phospho-ERK Signals, while SOS Induces Digital Signals in T and B Cell Lines and Primary T Cells

(A) Fluorescence flow cytometric analysis of ERK phosphorylation in 20,000 individual Jurkat T cells per histogram. Cells were stimulated for the indicated time intervals with a TCR stimulating antibody (1:500 dilution of C305). ERK phosphorylation initially occurs in a unimodal fashion and switches to a bimodal pattern (Hartigan's tests). Numbers inside the histograms represent the percentage of cells on either side of the divider.

(B) As in (A) but cells were stimulated with 25 ng/ml PMA (a DAG analog) for shorter time intervals. Note the gradual increase of phospho-ERK over time without bimodal patterns.

(C) The indicated DT40 B cell lines were weakly or strongly stimulated through their BCR for 3, 10, or 30 min or left unstimulated. "U" or "B" labels indicate unimodal or bimodal (Hartigan test). See Figure S24 for methods, additional data, and p values.

(D) Same as in (C), except cells were stimulated with PMA, either weak (10 ng/ml) or strong (60 ng/ml). See Figure S25 for additional data.

(E and F) Digital, TCR-induced ERK phosphorylation in CD4-positive lymph node T cells but analog PMA-induced ERK phosphorylation. Cells were stimulated by crosslinking their TCR in (E) or by PMA in (F). (A)–(F) are representative examples of two, three, three, two, three, and two independent experiments, respectively.

A very different dose-response curve (red curve in Figure 6A) is predicted by computer simulations where the initial RasGTP level was set to a large value, and then the responses to smaller stimulus levels were calculated. This is the predicted dose response for cells that are first robustly stimulated such that a high RasGTP level is realized, then the stimulus is quickly

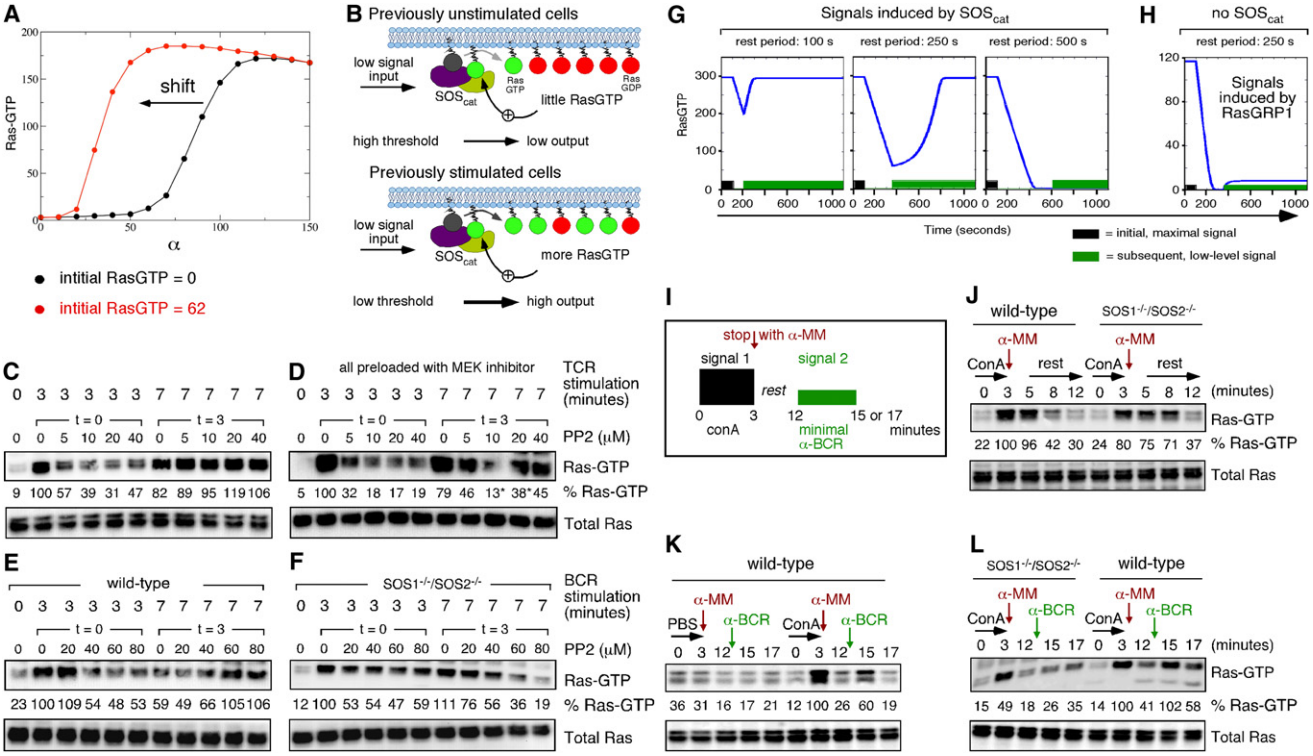

Figure 6. Hysteresis at the Level of RasGTP Depends on SOS

(A) Prediction of hysteresis in Ras activation from our stochastic simulation. Points in black and red denote Ras activations at a time t = 10 min when the cells had either 0 or 62 molecules/(μm)^2 of RasGTP concentrations at t = 0 min, respectively. All the simulations are done with a fixed RasGRP1 concentration at 500 molecules/(μm)^3.

(B) Cartoon illustrating the biochemical origin of hysteresis: a low level of remaining RasGTP that can bind the allosteric pocket in SOS.

(C–F) Analysis of GTP loaded Ras using pull-down assays. Lanes 3–6: Cells stimulated for 3 min in the presence of increasing amounts of PP2 (Src kinase inhibitor) added simultaneously with the stimulus at t = 0. Alternatively (lanes 8–11), cells were stimulated for 3 min, inhibitor was introduced at t = 3 min, and responses were analyzed at 7 min. Lane 1 is unstimulated, and lanes 2 and 7 have no inhibitor added. Legend of the panels: (C) Jurkat T cells and (D) Jurkat T cells preloaded with U0126 MEK1/2 inhibitor both stimulated with 1:500 diluted C305 (α-TCR), (E) WT DT40 B cells, and (F) SOS1$^{-/-}$SOS2$^{-/-}$ doubly deficient DT40 B cells both stimulated with 1:300 diluted M4 (α-BCR). Experiments presented in (C)–(F) are representative examples of three, four, five, and three independent experiments, respectively. Numbers indicate pixel intensity of the corresponding RasGTP, corrected for total Ras, one condition arbitrarily set at 100%. Due to a suboptimal blot transfer in (D), 13%* and 38%* are underrepresentations of the level of generated RasGTP.

(G) Modeling serial stimulation. RasGTP (blue line) was initially induced by high levels of SOS$_{cat}$ (black box, 350 molecules α). SOS$_{cat}$ was removed for 100, 250, or 500 s and subsequent low-level SOS$_{cat}$ signals were simulated (green box, 150 molecules α). Provided that RasGTP levels do not fall below the blue points (Figure 1C), robust restimulation is induced by low-level SOS$_{cat}$. The results are obtained from mean-field rate equations corresponding to the pathway in Figure 1B and the parameters in Table 1.

(H) Lack of sensitized restimulation in the absence of SOS. The model from Figure 1E is used to analyze a SOS-deficient state in the same manner as in Figure 6G. RasGRP1 values were set at 100 (black) and 50 (green) molecules of RasGRP1 in the simulation box, respectively. The response to the second stimulus is history independent.

(I) Experimental design to mimic serial stimulation of lymphocytes.

(J) Concanavilin A (Con A) induces RasGTP in WT DT40 and SOS1$^{-/-}$SOS2$^{-/-}$-deficient DT40 B cells. α-methyl mannoside (α-MM) is added at t = 3 min to stop the Con A-induced BCR stimulus (Weiss et al., 1987) and RasGTP levels decrease to slightly above basal levels at t = 12 min.

(K) Previous RasGTP induction by Con A stimulation of WT DT40 B cells followed by α-MM results in very sensitive induction of RasGTP by a second minimal BCR stimulus (1:4500 diluted M4; 1/15th of the amount in E and F), whereas priming with PBS as negative control does not.

(L) Induction of RasGTP by Con A in SOS1$^{-/-}$SOS2$^{-/-}$-deficient DT40 B cells does not result in sensitive RasGTP generation by a second signal (1:3000 diluted M4; α-BCR). Experiments presented in (J)–(L) are representative examples of three, four, and two independent experiments, respectively.

reduced (as in removal of antigen), and the response assessed after a time period that is sufficient for a new active Ras level to be established. When cells that have been previously robustly activated are exposed to lower stimulus levels, most SOS molecules have RasGTP bound to the allosteric site and are characterized by high GEF activity. So, for the same stimulus level (or SOS targeted to the membrane), previously stimulated cells will exhibit a higher level of active Ras than previously unstimulated cells because in the former situation SOS is a more active enzyme. Concomitantly, the threshold stimulus required for robust Ras activation shifts to lower values (Figures 6A and 6B) for previously stimulated cells. However, this hysteretic effect will only be manifested for a finite period of time. Ultimately, RasGTP molecules bound to the allosteric site of SOS in

previously stimulated cells will be displaced by RasGDP molecules as the amount of RasGTP in the cell declines because of lower stimulus levels. If the second stimulus level falls below a threshold, this process occurs very rapidly, and this is why hysteresis is not predicted for weak receptor stimulation.

SOS-Dependent Hysteresis in Ras Activation

Experimental results for Jurkat T cells and DT40 B cells (Figures 6C–6L) demonstrate the predicted hysteresis in Ras activation, and that it is due to the feedback loop associated with SOS and not due to feedback from downstream signaling modules.

Stimulation of Jurkat T cells using a maximal dose of TCR crosslinking antibody results in near maximal Ras activation after 3 min of stimulation (Figure S27A). Cells were also exposed to increasing concentrations of Src kinase inhibitor (PP2) to inhibit Lck (see Figure 4A) and interrupt signaling events upstream of Ras activation in a dose-dependent manner. PP2 was introduced simultaneously with the stimulus (t = 0 min) or after cells reached maximal levels of RasGTP (t = 3 min). RasGTP was analyzed at 3 min for PP2 added at t = 0 min. If PP2 was added at t = 3 min, RasGTP was assayed at 7 min, thereby allowing a new balance with the reduced stimulus to be established. Computer simulations (Figure S27D) show that this protocol should allow us to test whether hysteresis occurs at the level of Ras as predicted in Figure 6A.

Figure 6C shows that TCR-induced RasGTP levels in WT Jurkat cells decrease when PP2 is added simultaneously with the stimulus, demonstrating a dependence on Src kinases (or stimulus level) for RasGTP generation that is akin to the black curve in Figure 6A for previously unstimulated cells. However, when PP2 is added at 3 min (stimulus lowered after stimulation), RasGTP levels are high at 7 min even at high doses of PP2. This is akin to the red curve in Figure 6A and demonstrates hysteresis because, in previously stimulated cells, RasGTP levels are relatively high between 3 and 7 min in spite of a lower stimulus. After a sufficiently long time, as predicted, hysteresis is not observed (data not shown).

Importantly, these effects were not determined by feedback loops originating downstream of Ras. Preloading of cells with MEK1/2 inhibitor, U0126, efficiently blocks MEK and ERK phosphorylation but allows for RasGTP generation, albeit with slightly delayed kinetics (Figure S27A), but hysteresis was still observed (Figure 6D).

By using the doubly SOS-deficient DT40 cells, we also tested the prediction that SOS-mediated Ras activation underlies hysteresis. Maximal BCR crosslinking leads to similarly high levels of RasGTP at 3 min in WT and $SOS1^{-/-}SOS2^{-/-}$ cells (Figure S27B). Of note, RasGTP production is clearly impaired in moderately stimulated $SOS1^{-/-}SOS2^{-/-}$ cells (Figure S27C). RasGTP levels in WT DT40 cells were sensitive to PP2 inhibition at the initiation of BCR stimulation. When cells were allowed to generate RasGTP for the first 3 min prior to PP2 addition, hysteresis was observed since RasGTP levels were high when compared to cases where the same dose of PP2 was added at the initiation of BCR stimulation (Figure 6E). In sharp contrast, $SOS1^{-/-}SOS2^{-/-}$ cells do not exhibit hysteresis, and RasGTP levels decrease with increasing amounts of PP2 on the way up (PP2 at t = 0) and the way down (PP2 at t = 3) (Figure 6F).

Bistability and Hysteresis Provide Ras Signaling Memory during Serial Stimulation

T cell activation may require integration of membrane-proximal signals from sequential contacts (each approximately 3 min in duration) that occur between T cells and antigen-presenting cells (APCs) in lymphoid tissues (Bousso and Robey, 2003; Henrickson et al., 2008; Skokos et al., 2007). A molecular mechanism that enables T cells to "remember" past encounters with antigen is not known.

Suppose during a T cell-APC contact the quality and quantity of encountered pMHC ligands is sufficient to stimulate engagement of the SOS feedback loop and robust Ras activation but insufficient for other events necessary for T cell activation. The T cell disengages from the APC and is not subject to stimulation until it encounters another APC. During this period the stimulus is "off," and active Ras levels decline because phosphatases act on pLAT (Figure 4) causing SOS to disengage from the membrane, RasGAPs reduce RasGTP levels during the time that the stimulus is "off," etc. Suppose that during the next encounter of this T cell with an APC it encounters a weak stimulus that would not result in robust Ras activation if this T cell had not been previously robustly stimulated. We asked whether the existence of an underlying bistable steady-state structure due to feedback regulation of SOS (Figure 1) would result in restoration of robust Ras activation upon weaker restimulation. If so, bistability and hysteresis would be manifested as a molecular memory that enables integration of serially encountered weak signals after exposure to a strong stimulus.

To explore this idea, we carried out calculations with the minimal model shown in Figure 1. Robust stimulation of active Ras due to high levels of SOS_{cat} was followed by suddenly removing the stimulus. We then studied the dynamics of restimulation with a weak stimulus (green) after the originally strong stimulus has been "off" for a certain time (Figure 6G). Increasing the duration of the resting phase reduces the RasGTP level at the time of restimulation because of the RasGAPs present in our model. Figure 6G shows that maximal activation is recovered upon restimulation with a subsequent weaker stimulus, provided that RasGTP does not decline below the level of the unstable steady state (blue points in Figure 1C). If RasGTP levels decline to baseline during the duration when the stimulus is "off," then RasGTP levels are low upon restimulation (Figure 6G, 500 s rest period). If there is no bistability and hysteresis as when SOS_{cat} is not subject to feedback regulation (or Ras is activated via RasGRP), restimulation with a weak stimulus results in low levels of Ras activation regardless of prior stimulation, i.e., there is no memory (Figure 6H).

Stimulation of Jurkat T cells or B cells with the plant lectin Concanavilin A (Con A) results in robust calcium responses that rely on binding of Con A to the TCR or BCR (Weiss et al., 1987). Importantly, binding of Con A can be relatively rapidly abrogated by addition of α-methyl-mannoside (α-MM), a competitive carbohydrate. We used this protocol to test the predictions in Figures 6G and 6H. Because T and B cells respond similarly to this protocol, we used the DT40 system as it enables testing the effects of SOS by genetic deletion (Figure 6I).

Con A stimulation resulted in robust Ras activation in both WT and $SOS1^{-/-}SOS2^{-/-}$ DT40 B cells at 3 min (Figure 6J). Addition

of α-MM treatment to robustly stimulated WT cells resulted in a decline in RasGTP levels. It is important to note that at 12 min, RasGTP levels still remained moderately above the basal level. Next, we tested the effect of a very weak stimulus of anti-BCR crosslinking antibody given at this 12 min time point (see Figure 6K). Priming with Con A followed by α-MM treatment resulted in hyperresponsive RasGTP levels induced by this weak second signal that did not elicit a response when WT DT40 B cells were primed with PBS as a negative control (Figure 6K). In contrast, when doubly deficient SOS1$^{-/-}$SOS2$^{-/-}$ DT40 B cells were primed through the same regimen, we observed only minimal RasGTP stimulation by the second signal mediated by the BCR (Figure 6L). These data are consistent with the prediction (Figures 6G and 6H) that the underlying bistability and hysteresis due to feedback regulation of SOS confer memory to the dynamic responses of previously stimulated lymphoid cells.

DISCUSSION

Major Findings

We combined theoretical analyses and stochastic computer simulations to study membrane-proximal signaling in lymphocytes, with a view toward understanding how activation of a key signaling intermediate in diverse cell types (Ras) is regulated. Experimental tests of these predictions using diverse approaches and further in silico and in vitro studies lead to the following conclusions. A feedback loop associated with SOS-mediated Ras activation is necessary for digital signaling in lymphoid cells, and hysteresis in the dose-response curve for Ras activation. Digital signaling and hysteresis may also confer lymphocytes with short-term molecular memory of encounters with antigen (Figure 7). Alone, RasGRP-mediated Ras activation results in analog signaling in cell lines and lymph node T cells and does not exhibit hysteresis. But, intermediate levels of RasGRP activity lead to more efficient digital responses than with SOS alone. The interplay of differential activities of these two RasGEFs leading to efficient and varied cellular responses may be a principle that is employed more broadly and could have important implications for lymphocyte function. Our in silico and in vitro studies predict many phenomena that should be explored further.

Further Experimental Tests of Predicted Ras Signaling Characteristics

We have demonstrated that digital Ras-ERK signaling requires SOS in cells lines (Figure 5). Similar TCR-induced digital signals operate in primary T cells, but currently a direct demonstration of the involvement of SOS' positive feedback loop in primary cells is lacking. Future work to address this point will be aided by the generation of the appropriate mouse models.

Compartmentalized Ras signaling has received considerable recent interest (Campbell et al., 1998; Mor and Philips, 2006). SOS activates Ras exclusively at the plasma membrane, but RasGRP can also function on internal membranes. It will of interest to investigate how analog (RasGRP) and digital (SOS) mechanisms of Ras activation occur in time and space as well as whether recently observed spatial nanoclustering of active

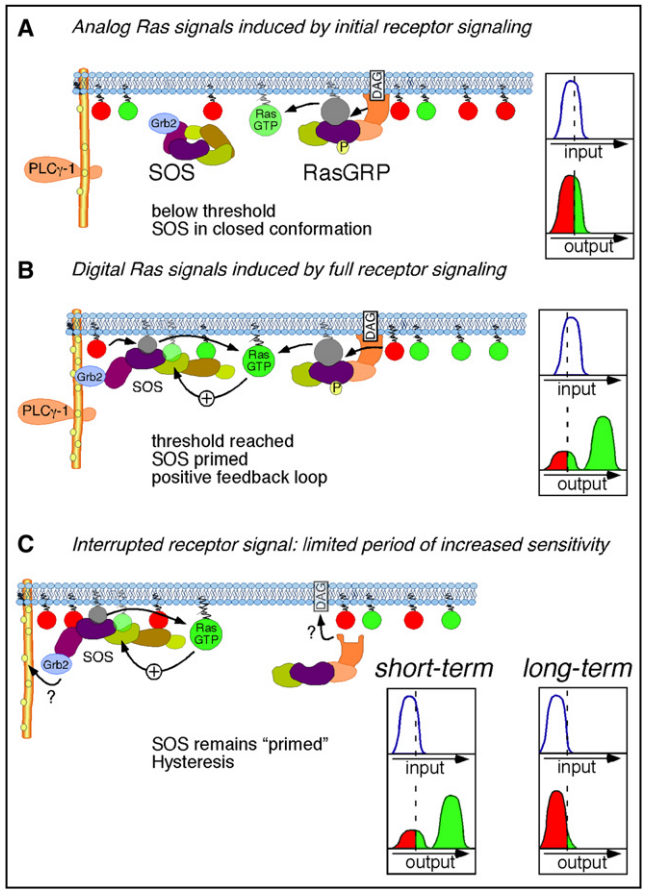

Figure 7. Model of Analog and Digital Signaling and Hysteresis in Lymphocytes

(A) Upon initial receptor activation analog Ras signals are generated in lymphocytes because Ras activation occurs solely via RasGRP. Inset: A small graded increase in signal input results in relatively low Ras output in an analog manner.

(B) Once a certain threshold in the analog receptor activation is surpassed, the output is characterized by digital Ras signals. Digital signals originate in the positive feedback loop that involves the allosteric pocket of SOS, initially primed by RasGTP coming from RasGRP, subsequently from both RasGRP and SOS.

(C) Previously stimulated cells maintain a limited period of increased sensitivity to activate Ras. The short-term hysteresis is caused by the low levels of RasGTP that remain but are potent in engaging the allosteric feedback loop. Inset: Short-term hysteresis provides a level of "signaling memory" in that a mild second signal can evoke a strong digital response because SOS molecules remain primed. However, hysteresis is limited and is lost long-term. The mechanisms of biochemical recruitment/retention of Grb2/SOS or RasGRP during hysteresis are unknown.

Ras proteins (Tian et al., 2007) is influenced by positive feedback regulation of Ras activation.

In other cell types, digital signaling has been reported to rely on a positive feedback loop between MAPK and phospholipase A_2 (Bhalla and Iyengar, 1999). Phospholipase A_2 is, however, not expressed in T and B lymphocytes (Gilbert et al., 1996). This may be why digital signaling in lymphocytes is controlled by feedback regulation of SOS' GEF activity. Nonetheless, feedback loops present in the MAPK pathway (Ferrell, 2002;

Kholodenko et al., 2002) undoubtedly further modulate our measurements of CD69 and ERK activation, and it will be important to examine how. Such investigations could help resolve puzzles such as why in SOS1$^{-/-}$SOS2$^{-/-}$ cells RasGTP levels are lower when PP2 is added after robust stimulation compared to when the inhibitor is added at t = 0, or why WT Jurkat and DT40 cells exhibit more pronounced hysteresis for higher doses of PP2 (Figure 6). These studies may also resolve whether delayed action of nuclear phosphatases that turn off ERK cause apparent hysteresis in ERK activation in SOS$^{-/-}$ DT40 cells without bistability (Figure S28).

Predicted Functional Implications of Digital Signaling and Hysteresis

The sharp threshold in the dose-response curve (i.e., digital signaling) originating from feedback regulation of SOS' GEF activity may provide an additional membrane-proximal checkpoint that prevents spurious T cell activation. Weak receptor stimulation could lead to low levels of TCR and ZAP-70 activation that do not efficiently recruit SOS to the membrane or produce sufficiently large levels of RasGTP via the RasGRP pathway. Thus, the SOS feedback loop will not ignite (Figure 7A), and the resulting low levels of downstream signaling will prevent spurious T cell activation in response to weak stimulation. In contrast, when receptor stimulation exceeds a threshold, the SOS feedback loop will be engaged resulting in a sharp/digital increase in downstream signaling. It has been suggested that digital ERK signaling, along with feedback regulation of Lck, may enable discrimination between ligands of varying potency (Altan-Bonnet and Germain, 2005).

If early signaling events do result in robust Ras activation, it would be undesirable to shut down signaling due to fluctuations in receptor-ligand binding. Hysteresis in the dose-response curve may stabilize signaling once it has proceeded past this checkpoint. We predict hysteresis to be observed for a finite time interval and for stimulus levels that are not far below the threshold. This may ensure that if the signal is absent for a sufficiently long time or falls below a threshold, signaling is terminated.

In vivo infections result in very low numbers of cognate peptide-MHC complexes on most APCs in lymphoid tissues. Recent studies have suggested that T cell activation in such circumstances requires integration of interrupted serial encounters with APCs bearing cognate ligands (Henrickson et al., 2008). Our results suggest that, if a T cell's membrane-proximal signaling machinery is robustly stimulated once, the short-term molecular memory conferred by feedback regulation of SOS (Figure 6) could enable subsequent weaker signals to robustly stimulate these cells, thereby enabling signal integration. This concept could be examined by combining intravital microscopy with imaging of signaling products such as Ras to test whether hysteresis during Ras activation plays a role in signal integration in vivo.

The threshold potency above which strongly binding ligands negatively select thymocytes in the thymus is very sharp while the positive selection threshold is graded (Daniels et al., 2006). This may be because negative selection results from strong signaling requiring active Ras levels that can be realized only upon ignition of the SOS feedback loop. The resulting digital response may correspond to the sharp boundary separating ligands that induce positive and negative selection in the thymus. Weak stimulation may only activate Ras via the RasGRP pathway, thereby eliciting purely analog responses during positive selection. This potential ability of RasGRP and SOS acting to mediate either analog or digital signaling that impacts T cell development needs to be further examined in mouse models developed with the aim of impairing analog or digital signaling.

EXPERIMENTAL PROCEDURES

Mean-Field Equations for the Minimal Model Shown in Figure 1

The minimal model is based on the following reactions shown in Figure 1A. The mass action rate equations corresponding to those reactions are

$$\frac{d[S]}{dt} = -k_1[S][R_D] + k_{-1}[SR_D] - k_2[S][R_T] + k_{-2}[SR_T] \tag{1A}$$

$$\frac{d[SR_T]}{dt} = k_2[S][R_T] - k_{-2}[SR_T] \tag{1B}$$

$$\frac{d[R_T]}{dt} = -k_2[S][R_T] + k_{-2}[SR_T] + \frac{k_3^{cat}[R_D][SR_T]}{K_{3m}+[R_D]} + \frac{k_4^{cat}[R_D][SR_D]}{K_{4m}+[R_D]} - \frac{k_5^{cat}[R_{GAP}][R_T]}{K_{5m}+[R_T]}. \tag{1C}$$

The total number of SOS and Ras molecules are conserved, which leads to the following constraints:

$$\alpha = [S] + [SR_D] + [SR_T]$$
$$\beta = [R_D] + [R_T] + [SR_D] + [SR_T].$$

In the above equations, [X] represents the concentration of the species, X. The abbreviations used for different species are as follows:

$$S \equiv SOS \quad R_D \equiv Ras - GDP \quad R_T \equiv Ras - GTP$$
$$SR_D \equiv SOS - Ras - GDP \quad SR_T \equiv SOS - Ras - GTP$$
$$R_{GAP} \equiv Ras - GAP$$

The Michealis constants are defined as $K_{3m} = (k_3^{cat} + k_{-3})/k_3$; $K_{4m} = (k_4^{cat} + k_{-4})/k_4$; $K_{5m} = (k_5^{cat} + k_{-5})/k_5$, where k_n, k_{-n} are the binding, unbinding rates of the substrate (S) to the enzyme (E), respectively, and k_n^{cat} is the rate of production of the product (P) from the complex (ES). The reaction is shown schematically below:

$$E + S \underset{k_n:k_{-n}}{\longleftrightarrow} ES \xrightarrow{k_n^{cat}} E + P.$$

K_{3m}, K_{4m}, and K_{5m} are calculated from Table S1. For the ordinary differential equations (ODE) in Equation 1A, reactions #1 and #2 in Table S1, for Equation 1B, reaction #2 in Table S1, and for Equation 1C, reactions #2, #3, #4, and #5 are used. For the reactions in #3, #4, and #5 in Table S1, we used the Michaelis Menten form, and the Michaelis constants are calculated from the binding, unbinding and the catalytic rates of the reactions as described above. In many cases, the K_D(= k_{off}/k_{on}) values are known for the reactions but the binding (k_{on}) and unbinding (k_{off}) rates are not known. Therefore, we carried out parameter sensitivity analyses, and our results are robust to up to 10-fold variations of the parameters. Details of this analysis are shown in Table S3. The left-hand sides of Equations 1A–1C are set to zero and the algebraic equations are solved for the steady-state concentrations.

Stochastic Simulations of the Model Shown in Figures 2 and 4

We used the Gillespie algorithm (Bortz et al., 1975; Gillespie, 1977; McAdams and Arkin, 1997) to perform stochastic simulations that effectively solve the Master equation (van Kampen, 1992) corresponding to the chemical reactions in the signaling network shown in Figure 2A. Simulation details and rather

exhaustive parameter sensitivity analyses are provided in the Supplemental Data (Sections II and III).

Cell Lines, Stimulations, Inhibitors, Plasmids, and Transfections

Human Jurkat leukemic T cells, chicken DT40 B cell lines, and derived lines were generated and cultured as described before (Oh-hora et al., 2003; Roose et al., 2005). Stimulations were done in PBS at 37°C with PMA, C305 (anti-TCRβ), or M4 (anti-BCR) or stimulated with Con A followed by α-MM treatment (Weiss et al., 1987). Cell lines were transfected as described before (Roose et al., 2005). For more details, see Supplemental Data, Section IV.

Western Blot Analysis and FACS Analysis

Protein expression was determined by western blot analysis of 1% NP40 lysates. Cell equivalents were analyzed per sample using the following antibodies: RasGRP1 (A176), Phospho-MEK1/2, Phospho-p44/42 MAP Kinase, Myc-tag (Cell Signaling), α-tubulin (Sigma), Ras (Upstate Biotechnologies), and Pan-Ras (Calbiochem) for detection of human or chicken Ras. Proteins were visualized using Western Lightning reagent plus (Perkin Elmer) and a Kodak Image Station 440CF and Kodak ID Image Analysis Software 3.5 to quantify expression levels. FACS assays were carried out as described before (Roose et al., 2005). For more details, see Supplemental Data, Section IV.

Ras Activation Assays

Activation of Ras was analyzed by a RasGTP pull-down assay essentially according to the manufacturer's instructions (Upstate). For more details, see Supplemental Data, Section IV.

SUPPLEMENTAL DATA

Supplemental Data include 31 figures, 13 tables, and Supplemental Experimental Procedures and can be found with this article online at http://www.cell.com/supplemental/S0092-8674(08)01631-0.

ACKNOWLEDGMENTS

We thank Dr. Kurosaki for DT40 lines and Dr. Dafna Bar-sagi for the H-RasG59E38 plasmid. We are grateful to Dr. DeFranco and members of the Weiss, Chakraborty, and Roose labs for critical reading of the manuscript. We apologize to colleagues we could not cite due to space constraints. Financial support: NIH Director's Pioneer Award and 1PO1/AI071195/01 (A.K.C.), the Howard Hughes Medical Institute as well as the Rosalind Russell Medical Research Center for Arthritis (A.W.), and the NCI (K01CA113367), Arthritis Foundation, and Sandler Foundation (J.P.R.).

Received: February 20, 2008
Revised: October 10, 2008
Accepted: November 24, 2008
Published: January 22, 2009

REFERENCES

Altan-Bonnet, G., and Germain, R.N. (2005). Modeling T cell antigen discrimination based on feedback control of digital ERK responses. PLoS Biol. *3*, e356. 10.1371/journal.pbio.0030356.

Barkai, N., and Leibler, S. (2000). Circadian clocks limited by noise. Nature *403*, 267–268.

Bhalla, U.S., and Iyengar, R. (1999). Emergent properties of networks of biological signaling pathways. Science *283*, 381–387.

Bortz, B., Kalos, M.H., and Lebowitz, J.L. (1975). J. Comput. Phys. *17*, 10–18.

Bousso, P., and Robey, E. (2003). Dynamics of CD8(+) T cell priming by dendritic cells in intact lymph nodes. Nat. Immunol. *4*, 579–585.

Boykevisch, S., Zhao, C., Sondermann, H., Philippidou, P., Halegoua, S., Kuriyan, J., and Bar-Sagi, D. (2006). Regulation of ras signaling dynamics by Sos-mediated positive feedback. Curr. Biol. *16*, 2173–2179.

Campbell, S.L., Khosravi-Far, R., Rossman, K.L., Clark, G.J., and Der, C.J. (1998). Increasing complexity of Ras signaling. Oncogene *17*, 1395–1413.

Corbalan-Garcia, S., Margarit, S.M., Galron, D., Yang, S.S., and Bar-Sagi, D. (1998). Regulation of Sos activity by intramolecular interactions. Mol. Cell. Biol. *18*, 880–886.

Daniels, M.A., Teixeiro, E., Gill, J., Hausmann, B., Roubaty, D., Holmberg, K., Werlen, G., Hollander, G.A., Gascoigne, N.R., and Palmer, E. (2006). Thymic selection threshold defined by compartmentalization of Ras/MAPK signalling. Nature *444*, 724–729.

Dower, N.A., Stang, S.L., Bottorff, D.A., Ebinu, J.O., Dickie, P., Ostergaard, H.L., and Stone, J.C. (2000). RasGRP is essential for mouse thymocyte differentiation and TCR signaling. Nat. Immunol. *1*, 317–321.

Ebinu, J.O., Stang, S.L., Teixeira, C., Bottorff, D.A., Hooton, J., Blumberg, P.M., Barry, M., Bleakley, R.C., Ostergaard, H.L., and Stone, J.C. (2000). RasGRP links T-cell receptor signaling to Ras. Blood *95*, 3199–3203.

Elf, J., and Ehrenberg, M. (2004). Spontaneous separation of bi-stable biochemical systems into spatial domains of opposite phases. Syst. Biol. (Stevenage) *1*, 230–236.

Ferrell, J.E. (2002). Self-perpetuating states in signal transduction: positive feedback, double-negative feedback and bistability. Curr. Opin. Cell Biol. *14*, 140–148.

Freedman, T.S., Sondermann, H., Friedland, G.D., Kortemme, T., Bar-Sagi, D., Marqusee, S., and Kuriyan, J. (2006). A Ras-induced conformational switch in the Ras activator Son of sevenless. Proc. Natl. Acad. Sci. USA *103*, 16692–16697.

Genot, E., and Cantrell, D.A. (2000). Ras regulation and function in lymphocytes. Curr. Opin. Immunol. *12*, 289–294.

Gideon, P., John, J., Frech, M., Lautwein, A., Clark, R., Scheffler, J.E., and Wittinghofer, A. (1992). Mutational and kinetic analyses of the GTPase-activating protein (GAP)-p21 interaction: the C-terminal domain of GAP is not sufficient for full activity. Mol. Cell. Biol. *12*, 2050–2056.

Gilbert, J.J., Stewart, A., Courtney, C.A., Fleming, M.C., Reid, P., Jackson, C.G., Wise, A., Wakelam, M.J., and Harnett, M.M. (1996). Antigen receptors on immature, but not mature, B and T cells are coupled to cytosolic phospholipase A2 activation: expression and activation of cytosolic phospholipase A2 correlate with lymphocyte maturation. J. Immunol. *156*, 2054–2061.

Gillespie, D.T. (1977). Exact stochastic simulation of coupled chemical-reactions. J. Phys. Chem. *81*, 2340–2361.

Gureasko, J., Galush, W.J., Boykevisch, S., Sondermann, H., Bar-Sagi, D., Groves, J.T., and Kuriyan, J. (2008). Membrane-dependent signal integration by the Ras activator Son of sevenless. Nat. Struct. Mol. Biol. *15*, 452–461.

Hartigan, J.A., and Hartigan, P.M. (1985). The dip test of unimodality. Ann. Stat. *13*, 70–84.

Henrickson, S.E., Mempel, T.R., Mazo, I.B., Liu, B., Artyomov, M.N., Zheng, H., Peixoto, A., Flynn, M.P., Senman, B., Junt, T., et al. (2008). T cell sensing of antigen dose governs interactive behavior with dendritic cells and sets a threshold for T cell activation. Nat. Immunol. *9*, 282–291.

Houtman, J.C., Yamaguchi, H., Barda-Saad, M., Braiman, A., Bowden, B., Appella, E., Schuck, P., and Samelson, L.E. (2006). Oligomerization of signaling complexes by the multipoint binding of GRB2 to both LAT and SOS1. Nat. Struct. Mol. Biol. *13*, 798–805.

Kholodenko, B.N., Kiyatkin, A., Bruggeman, F.J., Sontag, E., Westerhoff, H.V., and Hoek, J.B. (2002). Untangling the wires: a strategy to trace functional interactions in signaling and gene networks. Proc. Natl. Acad. Sci. USA *99*, 12841–12846.

Kussell, E., Kishony, R., Balaban, N.Q., and Leibler, S. (2005). Bacterial persistence: a model of survival in changing environments. Genetics *169*, 1807–1814.

Margarit, S.M., Sondermann, H., Hall, B.E., Nagar, B., Hoelz, A., Pirruccello, M., Bar-Sagi, D., and Kuriyan, J. (2003). Structural evidence for feedback activation by Ras.GTP of the Ras-specific nucleotide exchange factor SOS. Cell *112*, 685–695.

McAdams, H.H., and Arkin, A. (1997). Stochastic mechanisms in gene expression. Proc. Natl. Acad. Sci. USA *94*, 814–819.

Mor, A., and Philips, M.R. (2006). Compartmentalized Ras/MAPK signaling. Annu. Rev. Immunol. *24*, 771–800.

Oh-hora, M., Johmura, S., Hashimoto, A., Hikida, M., and Kurosaki, T. (2003). Requirement for Ras guanine nucleotide releasing protein 3 in coupling phospholipase C-gamma2 to Ras in B cell receptor signaling. J. Exp. Med. *198*, 1841–1851.

Prasad, A., Zikherman, J., Das, J., Roose, J.P., Weiss, A., and Chakraborty, A.K. (2009). Origin of the sharp boundary that discriminates positive and negative selection of thymocytes. Proc. Natl. Acad. Sci. USA, in press. 10.1073/pnas.0805981105.

Roose, J.P., Mollenauer, M., Gupta, V.A., Stone, J., and Weiss, A. (2005). A diacylglycerol-protein kinase C-RasGRP1 pathway directs Ras activation upon antigen receptor stimulation of T cells. Mol. Cell. Biol. *25*, 4426–4441.

Roose, J.P., Mollenauer, M., Ho, M., Kurosaki, T., and Weiss, A. (2007). Unusual interplay of two types of Ras activators, RasGRP and SOS, establishes sensitive and robust Ras activation in lymphocytes. Mol. Cell. Biol. *27*, 2732–2745.

Ruiz, S., Santos, E., and Bustelo, X.R. (2007). RasGRF2, a guanosine nucleotide exchange factor for Ras GTPases, participates in T-cell signaling responses. Mol. Cell. Biol. *27*, 8127–8142.

Skokos, D., Shakhar, G., Varma, R., Waite, J.C., Cameron, T.O., Lindquist, R.L., Schwickert, T., Nussenzweig, M.C., and Dustin, M.L. (2007). Peptide-MHC potency governs dynamic interactions between T cells and dendritic cells in lymph nodes. Nat. Immunol. *8*, 835–844.

Sondermann, H., Soisson, S.M., Boykevisch, S., Yang, S.S., Bar-Sagi, D., and Kuriyan, J. (2004). Structural analysis of autoinhibition in the Ras activator Son of sevenless. Cell *119*, 393–405.

Starr, T.K., Jameson, S.C., and Hogquist, K.A. (2003). Positive and negative selection of T cells. Annu. Rev. Immunol. *21*, 139–176.

Tian, T., Harding, A., Inder, K., Plowman, S., Parton, R.G., and Hancock, J.F. (2007). Plasma membrane nanoswitches generate high-fidelity Ras signal transduction. Nat. Cell Biol. *9*, 905–914.

Trahey, M., and McCormick, F. (1987). A cytoplasmic protein stimulates normal N-ras p21 GTPase, but does not affect oncogenic mutants. Science *238*, 542–545.

van Kampen, N.G. (1992). Stochastic Processes in Physics and Chemistry (Amsterdam: North-Holland).

Wang, D.Z., Hammond, V.E., Abud, H.E., Bertoncello, I., McAvoy, J.W., and Bowtell, D.D. (1997). Mutation in Sos1 dominantly enhances a weak allele of the EGFR, demonstrating a requirement for Sos1 in EGFR signaling and development. Genes Dev. *11*, 309–320.

Weiss, A., Shields, R., Newton, M., Manger, B., and Imboden, J. (1987). Ligand-receptor interactions required for commitment to the activation of the interleukin 2 gene. J. Immunol. *138*, 2169–2176.